

Characterizing single-molecule dynamics of viral RNA-dependent RNA polymerases with multiplexed magnetic tweezers

Kuijpers, Louis; van Laar, Theo; Janissen, Richard; Dekker, Nynke H.

DOI

[10.1016/j.xpro.2022.101606](https://doi.org/10.1016/j.xpro.2022.101606)

Publication date

2022

Document Version

Final published version

Published in

STAR Protocols

Citation (APA)

Kuijpers, L., van Laar, T., Janissen, R., & Dekker, N. H. (2022). Characterizing single-molecule dynamics of viral RNA-dependent RNA polymerases with multiplexed magnetic tweezers. *STAR Protocols*, 3(3), Article 101606. <https://doi.org/10.1016/j.xpro.2022.101606>

Important note

To cite this publication, please use the final published version (if applicable). Please check the document version above.

Copyright

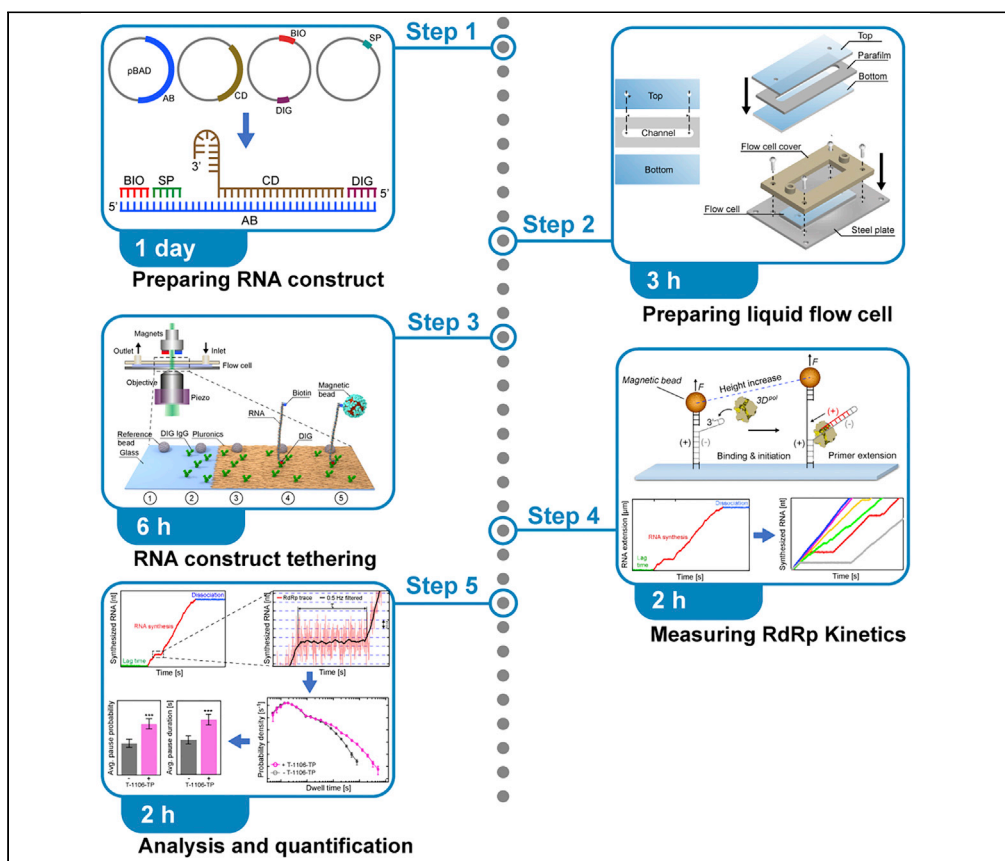
Other than for strictly personal use, it is not permitted to download, forward or distribute the text or part of it, without the consent of the author(s) and/or copyright holder(s), unless the work is under an open content license such as Creative Commons.

Takedown policy

Please contact us and provide details if you believe this document breaches copyrights. We will remove access to the work immediately and investigate your claim.

Protocol

Characterizing single-molecule dynamics of viral RNA-dependent RNA polymerases with multiplexed magnetic tweezers



Louis Kuijpers, Theo van Laar, Richard Janissen, Nynke H. Dekker

r.janissen@tudelft.nl (R.J.)
n.h.dekker@tudelft.nl (N.H.D.)

Highlights

Construction of a dsRNA molecule for probing single RdRp kinetics

Bias-free determination of kinetic parameters using dwell time analysis

Quantitative analysis of RNA synthesis dynamics by RdRp using magnetic tweezers

Protocol suitable for probing the effects of antiviral compounds that target RdRp

Multiplexed single-molecule magnetic tweezers (MT) have recently been employed to probe the RNA synthesis dynamics of RNA-dependent RNA polymerases (RdRp). Here, we present a protocol for simultaneously probing the RNA synthesis dynamics of hundreds of single polymerases with MT. We describe the preparation of a dsRNA construct for probing single RdRp kinetics. We then detail the measurement of RdRp RNA synthesis kinetics using MT. The protocol is suitable for high-throughput probing of RdRp-targeting antiviral compounds for mechanistic function and efficacy.

Publisher's note: Undertaking any experimental protocol requires adherence to local institutional guidelines for laboratory safety and ethics.

Kuijpers et al., STAR Protocols
3, 101606
September 16, 2022 © 2022
The Author(s).
<https://doi.org/10.1016/j.xpro.2022.101606>



Protocol

Characterizing single-molecule dynamics of viral RNA-dependent RNA polymerases with multiplexed magnetic tweezers

Louis Kuijpers,¹ Theo van Laar,¹ Richard Janissen,^{1,2,*} and Nynke H. Dekker^{1,3,*}¹Department of Bionanoscience, Delft University of Technology, 2629 HZ Delft, the Netherlands²Technical contact³Lead contact*Correspondence: r.janissen@tudelft.nl (R.J.), n.h.dekker@tudelft.nl (N.H.D.)
<https://doi.org/10.1016/j.xpro.2022.101606>

SUMMARY

Multiplexed single-molecule magnetic tweezers (MT) have recently been employed to probe the RNA synthesis dynamics of RNA-dependent RNA polymerases (RdRp). Here, we present a protocol for simultaneously probing the RNA synthesis dynamics of hundreds of single polymerases with MT. We describe the preparation of a dsRNA construct for probing single RdRp kinetics. We then detail the measurement of RdRp RNA synthesis kinetics using MT. The protocol is suitable for high-throughput probing of RdRp-targeting antiviral compounds for mechanistic function and efficacy. For complete details on the use and execution of this protocol, please refer to Janissen et al. (2021).

BEFORE YOU BEGIN

The presented assay allows a quantitative description of the RNA synthesis dynamics of viral RNA-dependent RNA polymerase, including the nucleotide incorporation rate, pausing frequency, and pause lifetimes under a variety of conditions (Janissen et al. (2021)). The assay further serves as a platform for the systemic screening of RdRp-targeting antivirals and their effects on RNA synthesis, which can be identified by changes in the processivity, pause frequency and pause duration (Janissen et al. (2021); (Seifert et al., 2021)). Due to the high spatiotemporal resolution of the presented technique, the assay can also be used to identify potential sequence motifs acting as copy-back recombination triggers (Janissen et al. (2021)).

The protocol is written for researchers with a working understanding of MT experimentation. This protocol, initially designed for the quantitative investigation of bacteriophage $\Phi 6$ RdRp dynamics (Dulin et al., 2015a), was modified for the RNA virus species enterovirus A71 (EV71) and poliovirus (PV) (Janissen et al., 2021). This protocol describes all steps for constructing the RNA template, setting up the MT experiment to measure RdRp RNA synthesis dynamics, and analysis of the RdRp translocation data. The protocol requires the RdRp of choice to be already purified (Fields et al., 1996), and the magnet distance-force relationship to be known (Ostrofet et al., 2018; Yu et al., 2014).

Preparation of the RNA construct

© Timing: 1 day

The following steps describe the construction of a dsRNA construct containing a short hairpin structure at the 3' overhang of the template strand for RdRp binding and primer extension. The dsRNA



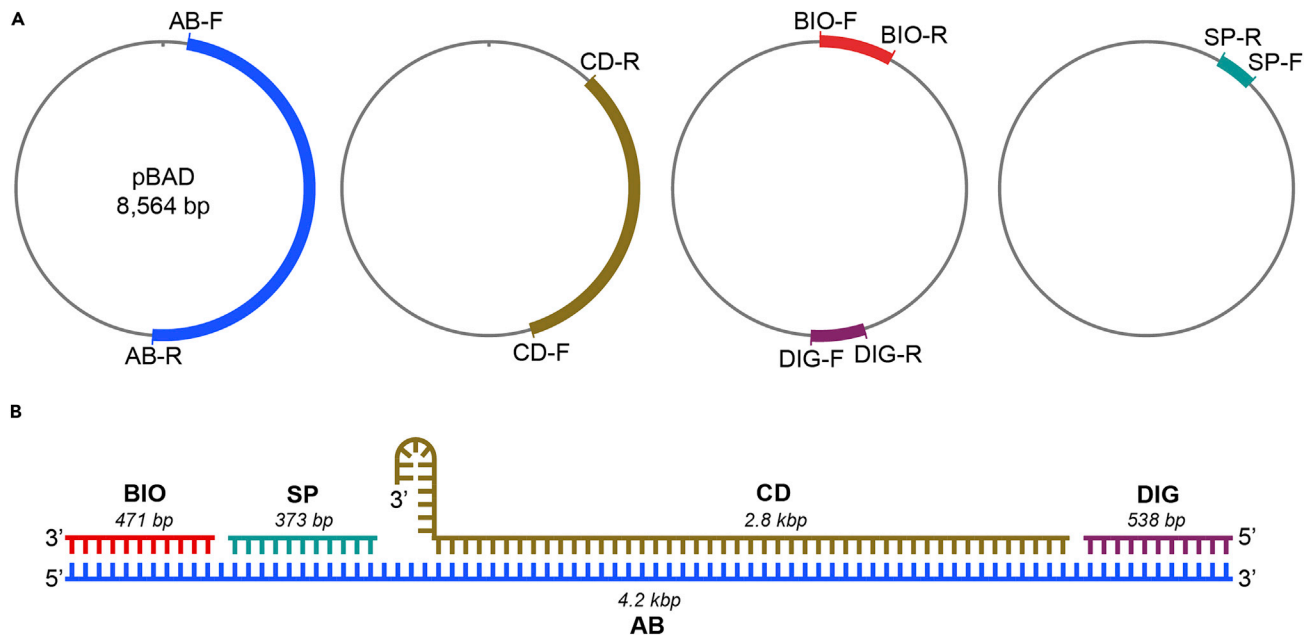


Figure 1. dsRNA construct preparation for the RdRp RNA synthesis assay

(A) Simplified pBAD plasmid maps for PCR amplification of the five DNA fragments.

(B) Annealing of the RNA transcripts to generate the dsRNA construct used in MT. The transcripts originate from run-off T7 transcription of the individual DNA fragments. BIO: biotin-enriched handle; DIG: digoxigenin-enriched handle; SP: spacer fragment; CD: RNA synthesis template; AB: construct backbone.

construct consists of five fragments initially amplified as DNA, then transcribed to generate RNA fragments that are annealed to obtain the full dsRNA construct (Figure 1).

1. The pBAD vector is subjected to gradient PCR with the primer combinations described in the KRT to produce the five DNA fragments (Figure 1). Only one primer in each combination contains a T7 promoter.

PCR reaction pipetting protocol

Reagent	Volume (μL)
Template (10 ng/ μL)	4
Primer F (10 μM)	4
Primer R (10 μM)	4
dNTPs (1 mM each)	4
5 \times HF buffer	32
MilliQ	110.8
Phusion polymerase	1.2

PCR cycle times

Steps	Temperature ($^{\circ}\text{C}$)	Time	Cycles
Initial Denaturation	98	2'30"	1
Denaturation	94	30"	29
Annealing	58	30"	
Extension	72	45"*	
Final extension	72	8'00"	1
Hold	20	1'00"	1

*For the extension step, use 45 s/kb of the fragment length. Fragment lengths are presented in Figure 1.

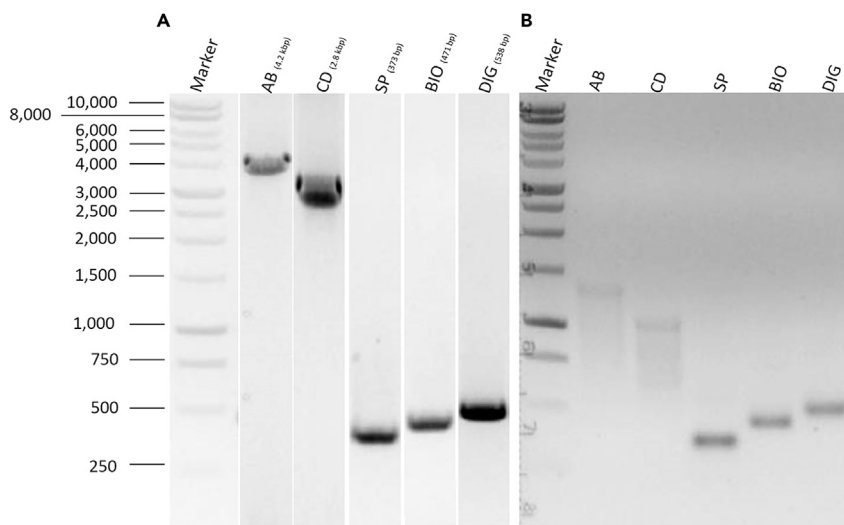


Figure 2. Agarose gels for verification of fragment size

(A) DNA fragments amplified by gradient PCR purified on individual 0.7% agarose gels (here, joined lanes), stained with SYBR Safe.

(B) Transcribed RNA products running on a 1.0% agarose gel, stained with SYBR Safe. AB: construct backbone; CD: RNA synthesis template; SP: spacer fragment; BIO: biotin-enriched handle; DIG: digoxigenin-enriched handle.

2. Load 20 μL of each DNA fragment into a lane of a 0.7% agarose gel, run for 60 min at 60 V, and purify them using gel electrophoresis (Figure 2A).
3. Stain the gel with SYBR Safe and visualize using blue light.
4. Cut the bands of each DNA fragment out of the gel and purify using the Promega Wizard kit according to the manufacturer's manual.
5. Determine the concentrations of the different DNA eluates with a spectrophotometer and adjust to 10 μM in MilliQ water.

Note: For the conversion of RNA concentration from $\text{ng}/\mu\text{L}$ to molar concentration, the following formula can be used:

$$\text{DNA (moles)} = \frac{m_{\text{dsDNA}} (\text{g})}{\left((l_{\text{dsDNA}} (\text{bp}) * \frac{607 \frac{\text{g}}{\text{mol}}}{\text{bp}}) + 158 \frac{\text{g}}{\text{mol}} \right)}$$

$$[\text{DNA}] (\text{M}) = \frac{\text{DNA (moles)}}{V (\text{l})}$$

with $m_{\text{dsDNA}} (\text{g})$ = mass of dsDNA in grams, $l_{\text{dsDNA}} (\text{bp})$ = length of dsDNA in base pairs, and $V (\text{l})$ = volume in liters.

6. For each DNA fragment, prepare the RNA transcription reaction using the Promega T7 transcription kit together with the appropriate pipetting protocol:

Note: Since RNases can cleave and degrade the RNA, we recommend the use of RNase free reagents and pipette tips from this point forward.

Transcription of fragments SP, CD, and AB

Transcription mixture	Volume (μL)
PCR product 250 ng	6
Transcription buffer (5 \times)	10

(Continued on next page)

Continued

Transcription of fragments SP, CD, and AB

Transcription mixture	Volume (μ L)
ATP (100 mM)	1
UTP (100 mM)	1
GTP (100 mM)	1
CTP (100 mM)	1
T7 polymerase	5
MilliQ water	25

Transcription of fragments BIO and DIG

Transcription mixture	Volume (μ L)
PCR product 250 ng	6
Transcription buffer (5 \times)	10
ATP (100 mM)	1
UTP (100 mM)	0.5
GTP (100 mM)	1
CTP (100 mM)	1
Bio-UTP/DIG-UTP (10 mM)	5
T7 polymerase	5
MilliQ water	20.5

7. Incubate the transcription reactions for 3 h at 37°C without shaking or rotation.
8. To each transcription mixture add 0.5 μ L DNaseI and incubate for another 15 min at 37°C.
9. Purify the synthesized RNA fragments with an RNeasy MinElute cleanup kit, following the [manufacturer's manual](#). Elute the RNA fragments in 1 mM sodium citrate (pH 6.4).
10. Confirm the RNA fragment size using a 1% agarose gel, run for 60 min at 60 V ([Figure 2B](#)).
11. Determine the concentration of the eluted RNA transcripts with a spectrophotometer.
12. To anneal the RNA transcripts to the dsRNA construct, mix the SP, CD, and AB RNA transcripts in equimolar ratio and add the DIG and BIO handles in 4 \times molar excess in SSC buffer (0.5 \times saline-sodium citrate) in a total reaction volume of 200 μ L.

Note: To obtain the force-extension relationship of ssRNA and dsRNA in MT, perform the same annealing reaction as in step 12, but without the CD fragment.

13. Perform the annealing reaction of the dsRNA or ssRNA constructs using the following program in the thermocycler:

Steps	Temperature ($^{\circ}$ C)	Time (min)	Cycles
Denaturation	65	60	1
Step-wise cooldown for annealing	-1.2	5	51
Hold	5	10	1

KEY RESOURCES TABLE

REAGENT or RESOURCE	SOURCE	IDENTIFIER
Antibodies		
Digoxigenin antibodies	Roche	RRID: AB_514496
Chemicals, peptides and recombinant proteins		
Hellmanex II or III	Sigma-Aldrich	Cat#Z805939
Ethanol	Honeywell	Cat#32221

(Continued on next page)

Continued

REAGENT or RESOURCE	SOURCE	IDENTIFIER
PBS	Sigma-Aldrich	Cat#P4417
Agarose	Sigma-Aldrich	Cat#A9539
SYBR Safe	Fisher Scientific	Cat#S33102
MilliQ	Millipore	Cat#ZWMQ22INEEO
SCC buffer (20x)	Promega	Cat#V4261
HEPES	Sigma-Aldrich	Cat#H3784
Pluronics® F127	Sigma-Aldrich	Cat#9003-11-6
BSA	Thermo Fisher Scientific	Cat#AM2616
NaCl	Sigma-Aldrich	Cat#S9888
MgCl ₂	Sigma-Aldrich	Cat#M8266
Dnasel	Thermo Fisher Scientific	Cat#EN0525
RdRp	Janissen et al. (2021)	N/A
ApU dinucleotide	IBA Lifesciences GmbH	Cat#0-31004
Biotin-16-UTP	Roche	Cat#14470528
Digoxigenin-11-UTP	Roche	Cat#14129222
rNTPs	GE Healthcare	Cat#27-2025-01
T1106 triphosphate	Blake Peterson lab	N/A
Ribavirin triphosphate	Jena Bioscience	Cat#NU-1105L
Superase RNase inhibitor	Thermo Fisher Scientific	Cat#AM2694
Polystyrene beads 1.50 µm	Polysciences	Cat#17133
Streptavidin-coated Superparamagnetic beads M280	Thermo Fisher Scientific	Cat#65001

Biological samples

RNA template	(Dulin et al., 2015b)	N/A
pBAD vector	Addgene	RRID: Addgene_37505

Software and algorithms

Labview 2011	National Instruments	RRID: SCR_014325
Igor Pro 6.37	WaveMetrics	RRID: SCR_000325
MATLAB	MathWorks	RRID: SCR_001622
MATLAB analysis algorithm	This study	https://doi.org/10.4121/19145426

Critical commercial assays

Promega Wizard Genomic DNA purification kit	Fisher Scientific	Cat#PR-A1120
RNeasy kit	QIAGEN	Cat#74004
Promega T7 RiboMAX Express Large Scale RNA Production system	Promega	Cat#P1320
Phusion High-Fidelity PCR Master Mix with HF Buffer	Thermo Fisher Scientific	Cat#F531S

Experimental models: Cell lines

RD cell line (one passage P1)	ATCC	RRID: CVCL_1649
-------------------------------	------	-----------------

Oligonucleotides

BIO-For	Biolegio	5'- AAGATTAGCGGATCCTACCTGAC
BIO-Rev	Biolegio	5'- TAATACGACTCACTATAGGA ACGGCTTGATATCCACTTTACG
SP-FOR	Biolegio	5'-TGCCATTCAAGGACTGCCG ATGTCGGTGCAGCCG
SP-REV	Biolegio	5'- TAATACGACTCACTATAGGAGCG CCGCTTCCATGTCCTGGAACGCT
CD-FOR	Biolegio	5'- ACGCTTTCGCGTACACCAACAGTT GTATGACGCTGGAAGCGATTCTGT
CD-REV	Biolegio	5'- TAATACGACTCACTATAGGCCGG ACGTTTCGGATCTTCGACATGCGC
DIG-FOR	Biolegio	5'- AGCGTAAAATTCAGTTCTTCGTGGCG
DIG-REV	Biolegio	5'- TAATACGACTCACTATAGGGCTAC CGGTTAACCTCAACTTCCATTTC

(Continued on next page)

Continued

REAGENT or RESOURCE	SOURCE	IDENTIFIER
AB-For	Biolegio	5'- TAATACGACTCACTATAGGATCGC CAAGATTAGCGGATCCTACCTGAC
AB-Rev	Biolegio	5'- GGTTAACCTCAACTTCCATTCC
Other		
Coplin Staining Jar	Polysciences	Cat#08415-3
Parafilm	VWR	Cat#291-0057
Flow cell holder	This work	https://doi.org/10.4121/19145426
Menzel-Gläser coverslips (#1, L x W = 24 x 60 mm)	VWR	Cat#631-1339
Sandblaster	PrepStart 200	Cat#212854
Sonicator	Fisher Scientific	Cat#13493609
Plasma-PREEN I	Plasmatic Systems Inc.	N/A
Reglo digital pump MS-2/8	Ismatec	Cat#ISM832
Thermo Thermal Cycler	Bio-Rad	Cat#1851148
NanoDrop	Fisher Scientific	N/A
Hot plate	Fisher Scientific	Cat#15353518

MATERIALS AND EQUIPMENT

SCC buffer (pH 7.0)

Reagent	Final concentration	Amount
SCC buffer (20x)	0.5x	2.5 mL
ddH ₂ O	N/A	97.5 mL
Total	N/A	100 mL

Store at 4°C for up to 3 months, heat to RT prior to use.

PBS buffer (pH 7.4)

Reagent	Final concentration	Amount
PBS	0.01 M Na ₂ PO ₄ buffer, 0.0027 M KCl, 0.137 M NaCl	1 tablet
ddH ₂ O	N/A	200 mL
Total	N/A	200 mL

Store at 4°C for up to 3 months, heat to RT prior to use.

Passivation buffer (pH 7.0)

Reagent	Final concentration	Amount
HEPES (1 M)	50 mM	5 mL
BSA (50 mg/mL)	1 mg/mL	2 mL
MgCl ₂ (1 M)	5 mM	500 μL
ddH ₂ O	N/A	92.5 mL
Total	N/A	100 mL

Store at 4°C for up to 3 months, heat to RT prior to use.

BSA buffer (pH 7.4)

Reagent	Final concentration	Amount
PBS	0.01 M Na ₂ PO ₄ buffer, 0.0027 M KCl, 0.137 M NaCl	1 tablet
BSA (50 mg/mL)	40 μg/mL	1.6 mL
ddH ₂ O	N/A	198.4 mL
Total	N/A	200 mL

Store at 4°C for up to 3 months, heat to RT prior to use.

Preparation buffer (pH 7.4)

Reagent	Final concentration	Amount
HEPES (1 M)	50 mM	5 mL
NaCl (1 M)	150 mM	15 mL
BSA (50 mg/mL)	20 μ g/mL	40 μ L
F127 (5%)	0.02%	400 mg
ddH ₂ O	N/A	80 mL
Total	N/A	100 mL

Store at 4°C for up to 3 months, heat to RT prior to use.

Transcription buffer (pH 6.6)

Reagent	Final concentration	Amount
HEPES (1 M)	50 mM	5 mL
MgCl ₂ (1 M)	5 mM	500 μ L
BSA (50 mg/mL)	125 μ g/mL	250 μ L
F127 (5%)	0.02%	400 μ L
DTT (100 mM)	1 mM	1 mL
Superase (20 U/ μ L)	0.1 U/ μ L	500 μ L
ddH ₂ O	N/A	92 mL
Total	N/A	100 mL

Store at 4°C for up to 3 months, heat to RT prior to use.

STEP-BY-STEP METHOD DETAILS

Preparation of the flow cell

⌚ Timing: 2.5 h

1. Use a sandblaster, CNC laser cutter, or diamond drill to drill two holes (~1.0–1.5 mm diameter) into the top cover slip for the inlet and outlet of the flow cell; see [Figure 3A](#).
2. Cut a double-layer of parafilm with a scalpel to the desired channel dimensions (here, 5 mm wide and 40 mm long; see also [Figure 3A](#)).
3. Clean a (top) coverslip with holes (obtained at step 1) and a (bottom) coverslip without holes by sonicating them for 25 min in 4% (v/v) Hellmanex III in MilliQ water at 40°C in a coplin staining jar.
4. Wash the coverslips multiple times with MilliQ water.
5. Sonicate the coverslips for 25 min in MilliQ water at 20°C.
6. Sonicate the coverslips for 25 min in Ethanol (e.g., *pro analysis* grade).
7. Dry the coverslips with a nitrogen stream.
8. Apply oxygen plasma to both coverslips (20 s, oxygen flow: 2.5 SCFH; 200 W).
9. Assemble the flow cell by melting the double-layer of parafilm between the top and the bottom coverslip on a hot plate (95°C for 30 s; see also [Figure 3B](#)).

Note: It is recommended to prepare multiple coverslips for higher throughput or in case of leakage/breaking of flow cells.

Flow cell assembly

⌚ Timing: 30 min

The flow cell holder ensures proper attachment to the magnetic tweezers, minimizing potential vibrational influence and mechanical drift to measurement accuracy. Additionally, it adds practical inlet and outlet connections to the flow cell.

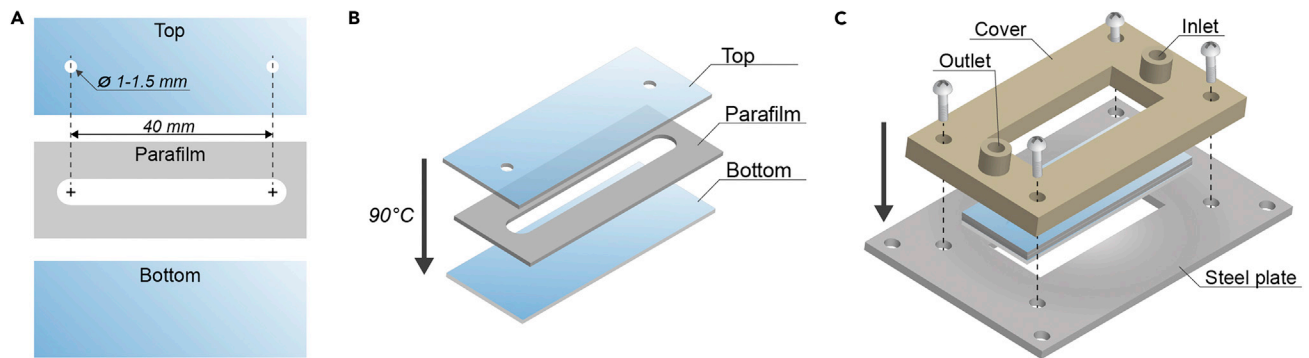


Figure 3. Flow cell assembly process

(A) A flow cell consists of a top coverslip with two holes of 1–1.5 mm diameter, approximately 40 mm from each other, a double layer of parafilm (~200 μm thickness) with cut-out channel in the center, and a bottom coverslip. The total volume of the flow cell channel corresponds to ~70 μL .

(B) Representation of flow cell assembly by melting the double-layer of parafilm between the top and bottom coverslips.

(C) Assembly of the flow cell in an MT flow cell holder. The technical drawings of the MT flow cell holder parts are available at <https://doi.org/10.4121/19145426>.

10. Assemble the flow cell in a flow cell holder (Figure 3C).
11. Attach the flow cell to the magnetic tweezers instrument and attach the outlet to a tube that is connected to a peristaltic pump (Figure 3C).

Note: Any pump type (e.g., peristaltic, syringe) can be used as long as speeds as low as ~200 $\mu\text{L}/\text{min}$ can be achieved.

12. Flow 300 μL PBS buffer through the flow cell by pipetting the solution directly into the inlet (Figure 3C) during pumping and assure full wetting (complete side-to-side covering of the channel with buffer within the flow cell).

Note: Throughout the protocol it is important to have all buffers at least at 20°C and use low flow rates (e.g., ~200 $\mu\text{L}/\text{min}$) to minimize the formation of air bubbles in the flow cell. Additionally, prior degassing of the buffers can be beneficial.

13. Perform a leakage test by closing the valve to the pump, filling the inlet with buffer, and observing the reduction in volume at the inlet for ~15 min. A large reduction in volume indicates leakage.

Note: Evaporation will also reduce the volume, but only marginally over time. If leakage is apparent, it might be resolved using one of the presented solutions (Troubleshooting; Problem 1: the flow cell).

Attachment of reference beads to flow cell surface

⌚ Timing: 15 min

Reference bead attachment to the surface provides a reference point for displacement of the magnetic beads relative to the surface.

14. Flow 100 μL of polystyrene beads (stock concentration of 1.35×10^{10} beads/mL) diluted 1,500 times in PBS into the flow cell (see Figure 4: step 1).
15. Incubate solution until 5–8 beads per field of view are adhered to the surface.
16. Flush all non-adhered beads out using 1–2 mL PBS buffer.

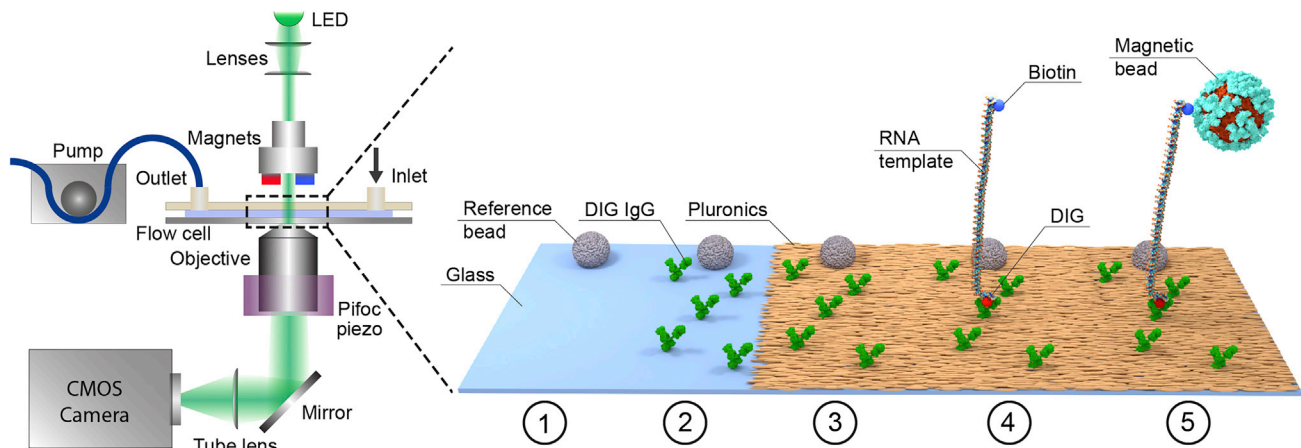


Figure 4. Schematic of the MT and step-wise functionalization of the flow cell surface

(Left) General overview of the MT setup: light originating from an LED travels through the gap between the magnets, illuminates the flow cell, and is captured by the objective. The images are reflected to and recorded by a CMOS camera and analyzed with custom-written software to determine the x, y and z positions of the magnetic beads in real time (Cnossen et al., 2014). The outlet of the flow cell holder is connected to a suction pump. (Right) The steps involved in coating the flow cell surface and tethering the RNA construct: (1) Reference beads are attached to the surface. (2) Anti-DIG antibodies are attached to the surface, serving as an anchor for the RNA construct. (3) Passivation of the glass surface using the poloxamer Pluronic F127 to suppress unspecific adhesion of biomolecules and magnetic beads. The antibodies and reference beads protrude through the surface coating. (4) The RNA construct is anchored to the flow cell via anti-DIG: DIG linkage. (5) A streptavidin-coated magnetic bead is attached to the RNA construct through the strong biotin:streptavidin interaction. Drawings are not to scale.

Attaching digoxigenin antibodies to the flow cell surface

⌚ Timing: 70 min

The digoxigenin antibodies provide the RNA construct an anchor point on the surface.

17. Flush 100 μ L of 0.1 mg/mL anti-DIG IgG in PBS into the flow cell and incubate for 1 h (see [Figure 4](#): step 2).
18. Flush out non-adhered, residual anti-DIG IgG using 500 μ L PBS buffer.

Surface passivation with BSA and F127

⌚ Timing: 170 min

Surface passivation ensures that non-specific adhesion of proteins, RNA, or magnetic beads is reduced to a minimum.

19. Flush through the flow cell 500 μ L of PBS supplemented with 10 mg/mL BSA (see [Figure 4](#): step 3).
20. Incubate for 2 h.
21. Flush through the flow cell 500 μ L BSA buffer.
22. Flush through the flow cell 500 μ L of PBS supplemented with 0.5% F127.
23. Incubate for 30 min.
24. Flush through the flow cell 500 μ L PBS.

Washing of magnetic beads

⌚ Timing: 10 min

Washing the magnetic beads in passivation buffer ensures that non-specific adhesion of magnetic beads to the surface is reduced to a minimum. Furthermore, it allows for a buffer exchange from the manufacturer's storage buffer.

Note: The washing of the magnetic beads can be performed in parallel to the surface passivation. We advise to perform the steps 25–27. during the incubation of 0.5% F127 in the flow cell (step 23).

25. Add 3.0 μL of M280 magnetic beads to 100 μL of passivation buffer.
26. Mix the solution, then separate the magnetic beads from the liquid using a magnetic stand and discard the supernatant.
27. Repeat previous step 2 more times with fresh passivation buffer. Afterwards, resuspend the magnetic beads in 100 μL preparation buffer.

RNA tethering between surface and magnetic beads

⌚ Timing: 35 min

RNA and magnetic bead tethering are crucial for setting up the MT assay.

28. Inject 100 μL of 2 pM RNA construct in preparation buffer into the flow cell (see [Figure 4](#): step 4).

Note: For the conversion of RNA concentration from $\text{ng}/\mu\text{L}$ to M, the following formula can be used:

$$\text{RNA (moles)} = \frac{m_{\text{dsRNA}} (\text{g})}{\left((l_{\text{dsRNA}} (\text{bp}) * \frac{641 \frac{\text{g}}{\text{mol}}}{\text{bp}}) + 318 \frac{\text{g}}{\text{mol}} \right)}$$

$$[\text{RNA}] (\text{M}) = \frac{\text{RNA (moles)}}{V (\text{l})}$$

with $m_{\text{dsRNA}} (\text{g})$ = mass of dsRNA in grams, $l_{\text{dsRNA}} (\text{bp})$ = length of dsRNA in base pairs, and $V (\text{l})$ = volume in liters.

29. Incubate for 20 min.
30. Flush 500 μL of preparation buffer through the flow cell to wash away non-tethered RNA constructs.
31. Inject 100 μL of washed magnetic beads and incubate until 200–300 beads are tethered per field of view, typically after ~ 5 min (here, the field-of-view dimensions are $491 \mu\text{m} \times 369 \mu\text{m}$; see [Figure 4](#): step 5).

Note: For this protocol we recommend using M280 beads because they can readily reach forces up to tens of pN, and their hydrophobic surface coating significantly reduces non-specific bead adhesion on the surface compared to hydrophilic M270 beads.

Note: If unspecific bead adhesion to the surface is apparent, it might be resolved using one of the presented solutions ([Troubleshooting](#); [Problem 3](#): all magnetic beads are adhered to the surface).

32. Wash surplus of untethered beads out using 1–2 mL of preparation buffer.

Note: The magnetic beads should be held at a constant force of ≥ 2 pN to exclude potential non-specific bead adhesion on the surface before the initiation of RNA synthesis.

Note: If tether formation is not observed, it might be resolved using one of the presented solutions ([Troubleshooting](#); [Problem 2](#): absence of tether formation).

Creating a magnetic bead Z-lookup table

⌚ Timing: 5 min

Bead Z-position lookup tables are created as a reference to accurately determine the beads' vertical position relative to the focal plane over time. There are different ways to determine the bead Z-position in MT. Here, we create an individual look-up table for each dsRNA-tethered bead and reference bead ([Cossen et al., 2014](#); [Gosse and Croquette, 2002](#)).

33. Create bead Z-position look-up tables (200 steps, 50 nm step size) at a constant force of 10 pN.

Measuring the force extension curves for dsRNA and ssRNA

⌚ Timing: 30 min

This measurement has to be made only once to estimate the extensions of the dsRNA and ssRNA (created by annealing all fragments with the exception of the CD fragment ([Figure 1B](#)) according to [before you begin](#), step 12) constructs as a function of force. This information will be important at later stage to convert the height change of the tethered beads in micrometers to nucleotides synthesized by RdRp.

34. Measure the extension of dsRNA and ssRNA with force ranging from 0.01 to 40 pN.

35. Repeat steps 1–34. using the ssRNA construct (without CD transcript).

36. Determine the ssRNA $l_{ss}(F)$ and dsRNA $l_{ds}(F)$ extensions. Select the lowest possible force at which the the difference between $l_{ss}(F)$ and $l_{ds}(F)$ is sufficiently large. Larger differences between $l_{ss}(F)$ and $l_{ds}(F)$ will result in a larger bead displacement in l-direction per nucleotide incorporated by the RdRp, and thus an increased spatial resolution. For the RNA constructs used here, 25 pN was chosen; see also [Figure 5](#).

Ternary complex formation

⌚ Timing: 30 min

Ternary complex formation is the construction of the full RNA tether with a stalled RdRp present on the RNA template. Ternary complex formation can significantly increase RdRp re-initiation efficiency when dinucleotide ApC is used.

37. Flush 80 μ L of transcription buffer supplemented with 600 nM RdRp, 0.6 mM ATP, 0.6 mM CTP and 1.2 mM ApC dinucleotide into the flow cell.

38. Incubate for 20 min.

39. Wash out all non-bound RdRp with 500 μ L of transcription buffer.

RNA tether characterization

⌚ Timing: 15 min

It is important to verify that the dsRNA constructs are singly tethered to a magnetic bead and of correct length. Furthermore, the measured length of each dsRNA tether must be known to convert the reduction in bead height upon RdRp RNA synthesis from micrometers to transcribed RNA nucleotides. The recording of the magnetic bead movement in all three dimensions was conducted with

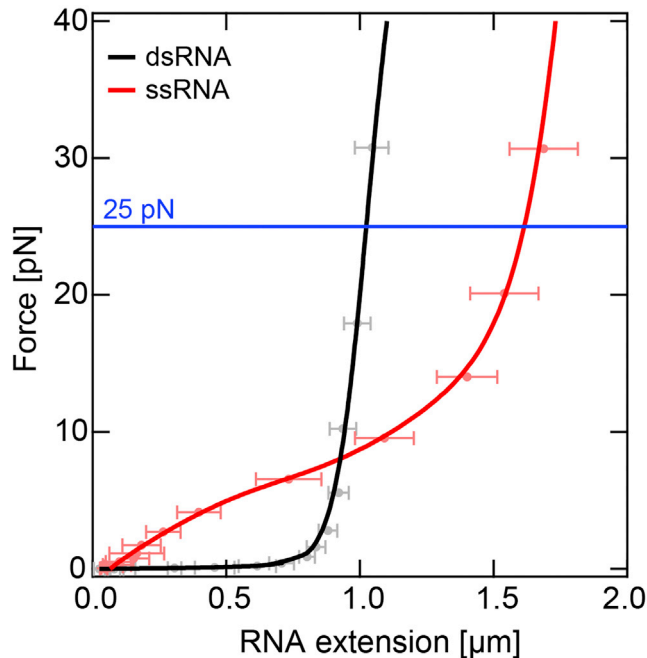


Figure 5. Force-extension curves of ssRNA and dsRNA

Force-extension curve of the dsRNA construct (gray) and the ssRNA construct (red) that lacks the CD fragment. The lines represent a WLC fit to the dsRNA data (black) and a linear interpolation of the ssRNA data (red). During RdRp RNA synthesis, the CD template strand is displaced from the AB strand, gradually increasing the fraction of ssRNA. A constant force of 25 pN (blue) was selected for our experiments due to the large difference in extension between dsRNA and ssRNA, which provides high spatial resolution for RdRp RNA synthesis. Error bars represent standard deviation ($N = 8$).

the control software described and published in [Clossen et al. \(2014\)](#). The measurement parameters were set to: 25 Hz camera frequency, Look Up Table (LUT) range of 10 μm with steps of 50 nm, *quadrant interpolation* as the algorithm used for the bead's Z-position determination, and a Region of Interest (ROI) of 90 px.

40. Start the data acquisition and perform the dsRNA tether characterization by changing the force and magnet rotation over time (see also [Figures 6A and 6B](#)) as follows:

Characterization of dsRNA tether

Magnet action	Force (pN)	Rotation (turns)	Time (s)	Purpose
Magnet height	0	0	5	Determine z-offset (z_0)
Magnet height	25	0	10	Stretch tether to measurement force
Magnet rotation	25	-30	10	Probe for multiple DNA tethering
Magnet rotation	25	0	10	Return to original rotation state
Magnet rotation	25	2	8	Determine DNA attachment to bead
Magnet rotation	25	-2	16	Return to original rotation state
Magnet height	3	0	5	Relax tether, maintaining low force

Note: The undesired tethering of multiple RNA tethers to one bead is signified by a sharp decrease in the bead I-position during the rotation of the magnets in the negative direction at high force. Additionally, the rotations provide information instrumental to the determination of the length of the RNA tether, see below.

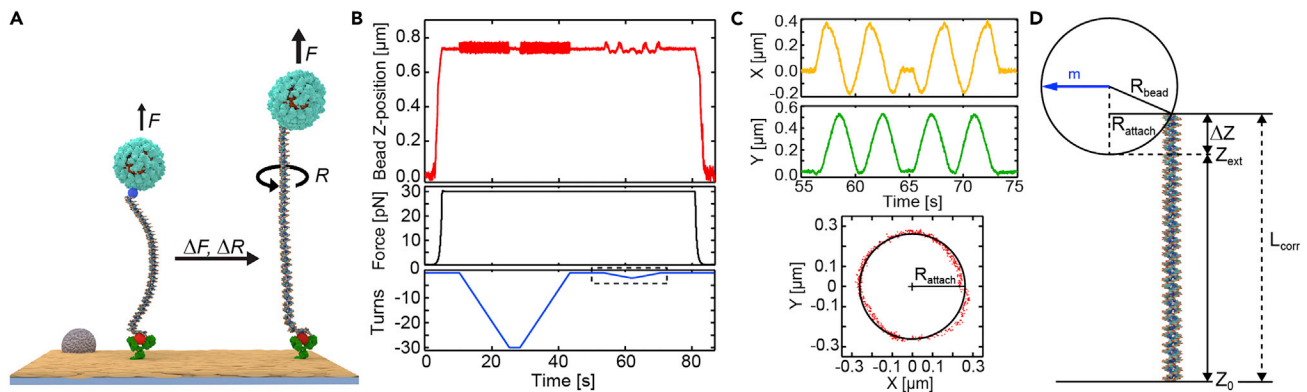


Figure 6. dsRNA tether characterization measurement and analysis

(A) The dsRNA tether is stretched from low to high force (ΔF) as well as rotated (ΔR) with a varying speed and number of turns.
 (B) Bead Z-position at zero force (top; red) and applied force (middle; black) during the experiment (here, 25 pN), allowing the determination of the apparent end-to-end length (L_{app}) of the dsRNA tether. The magnet is rotated (bottom; blue) to determine whether the dsRNA is singly tethered to the magnetic bead (with -30 turns at the force applied for the RNA synthesis experiment), and to assess the distance R_{attach} between the off-center attachment point of the dsRNA tether and the bead's geometric south pole (as defined when the bead's net magnetic moment (m) aligns with the field, panel D).
 (C) X- and Y-positions of the magnetic bead during slow rotations (0.25 s/turn; see the dashed box in (B)) allow the determination of R_{attach} using a circular fit.
 (D) The correct end-to-end dsRNA construct length L_{corr} is the sum of the apparent length Z_{ext} and ΔZ , where ΔZ is the height difference between the off-center dsRNA attachment point.

41. From the traces, determine each the magnetic bead's height at zero force (Z_0) and at 25 pN (Z_{ext}); see [Figure 6B](#).
42. Determine the radius of the magnetic beads' rotational motion R_{attach} by fitting the plot of X-positions in function of Y-positions with a circle; see [Figure 6C](#).

Note: The attachment point of the RNA tether to the magnetic bead is in most instances not perfectly at the bead's geometric south pole ([Figure 6D](#)) ([Klaue and Seidel, 2009](#); [Lipfert et al., 2009](#)). Therefore, the apparent length of tether (Z_{ext}) can be significantly smaller than the actual tether length (L_{corr}) and needs to be corrected. Slow rotation of the bead will provide crucial information for the correction. While we used Igor Pro (V6.37) as the software platform for the analysis of the bead traces, any other scripting-capable software that is able to import the text file output of the data acquisition software can be used, i.e., commonly used MATLAB and Python.

43. Calculate the length difference ΔZ between the RNA attachment point R_{attach} and the bead's south pole using the bead radius R_{bead} and the Pythagorean theorem (see also [Figure 6D](#)):

$$\Delta Z = R_{bead} - \sqrt{R_{bead}^2 - R_{attach}^2}$$

44. Add the corrected tether length by adding ΔZ to the apparent end-to-end length Z_{ext} obtained from the calibration measurement (see [Figure 6D](#)):

$$L_{corr} = Z_{ext} - Z_0 + \Delta Z$$

45. Calculate the average length of an RNA base by dividing L_{corr} by the number of base pairs in the construct; this value is later used to convert changes in bead Z-position to synthesized RNA products as a function of time.

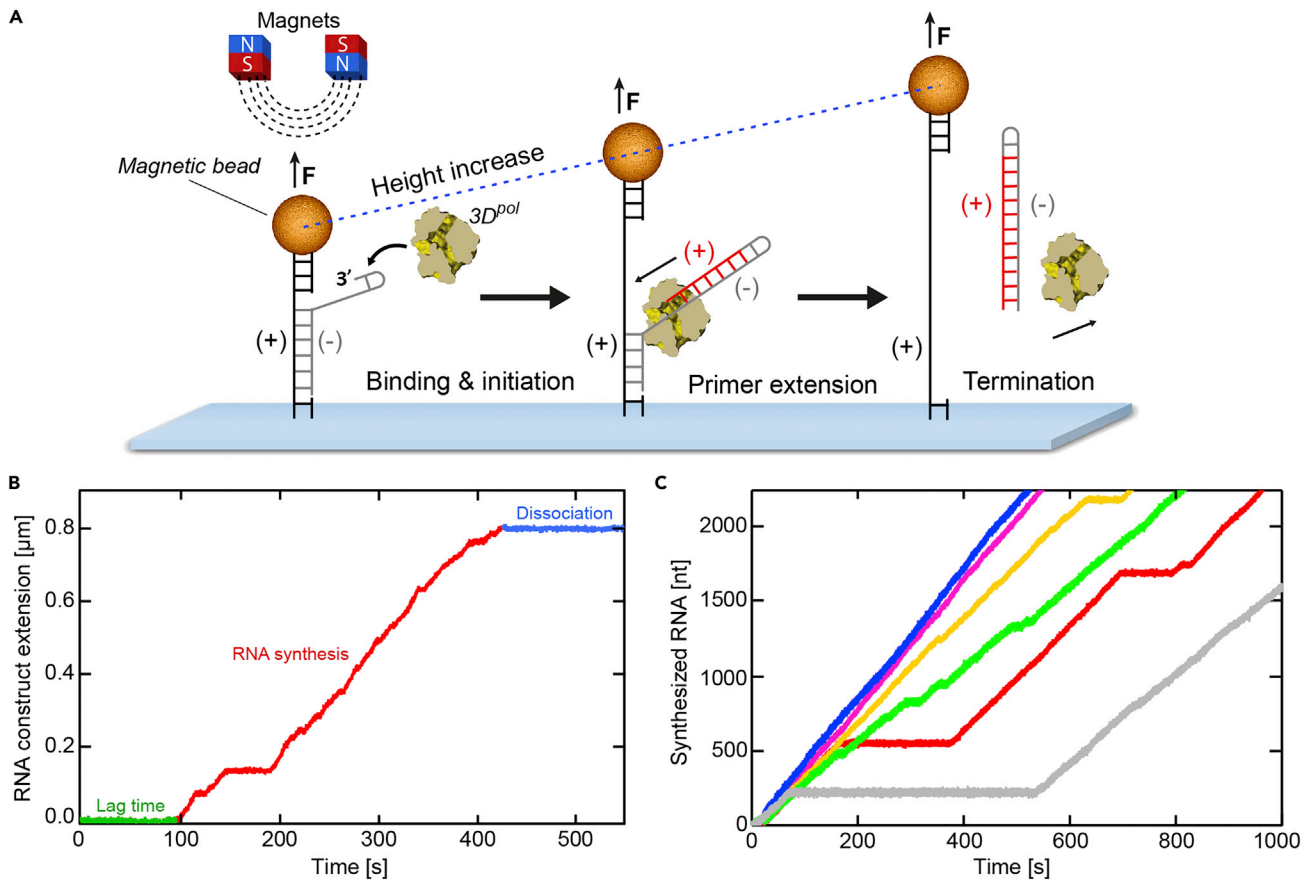


Figure 7. Processing of RNA synthesis trajectory data

(A) Schematic of the single-molecule (+)-strand RNA synthesis assay, showing binding of an RdRp to a hairpin at the 3' end of the (-)-strand (gray) of the surface-attached RNA construct. A magnetic bead attached to the RNA construct is subject to a constant force of 25 pN during RNA synthesis. Primer extension (red) from the 3' end of hairpin will lead to displacement of the template RNA (gray) from the tethered RNA (black). At 25 pN force, conversion of dsRNA to ssRNA causes a corresponding increase in the distance of the magnetic bead from the surface.

(B) Non-processed RdRp RNA synthesis example trajectory, normalized to the initial RNA extension prior NTP-addition. The lag time (green) is the time that the RdRp is inactive before re-initializing RNA synthesis upon NTP-addition and can vastly differ between RdRps. RNA synthesis (red) is intermittent, with stochastic pauses of different lifetimes. Arrest or dissociation of the RdRp causes the RNA extension (or bead z-position) to stop changing (blue).

(C) Superimposed, processed example RNA synthesis trajectories that were cut and converted to RNA nucleotides synthesized (data sets from (Janissen et al., 2021)).

Measuring RdRp RNA synthesis kinetics

⌚ Timing: 2 h

Addition of all nucleotides allows the ternary complexes to re-initiate RdRp RNA synthesis (Figure 7A).

46. Lower the magnet to the appropriate height to apply a constant force of 25 pN (or any other force determined in steps 34–36).
47. Re-initiate RNA synthesis by flushing 100 μ L of transcription buffer supplemented with all four rNTPs into the flow cell (the NTP concentration depends on the experiment design; here, 1 mM was chosen).
48. Immediately after, start the measurement and record all magnetic bead Z-positions for 2 h.

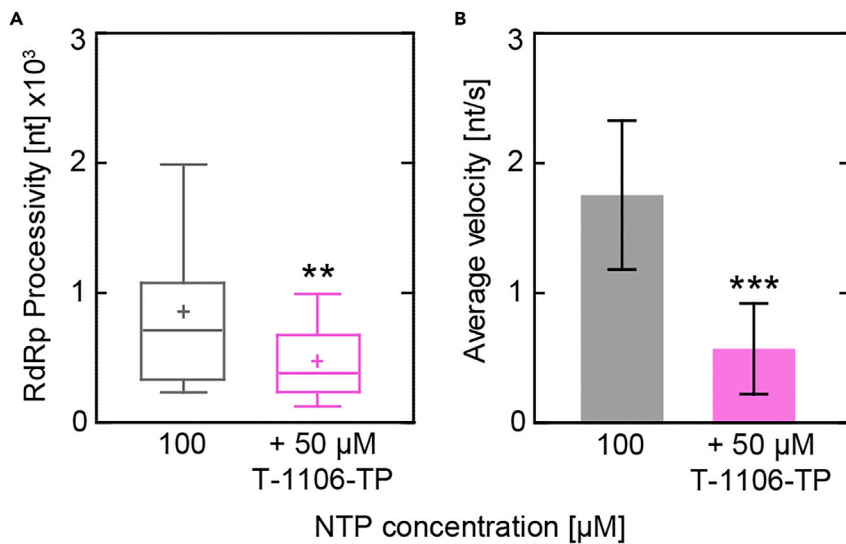


Figure 8. RdRp processivity and average RNA synthesis velocity of EV-A71 RdRp
(A and B) (A) RdRp processivity and (B) average RNA synthesis velocity (mean \pm SD) derived from example EV-A71 RdRp trajectories in the absence and presence of T-1106 triphosphate (data sets from (Janissen et al., 2021)). Statistical analyses were performed using unpaired, two-tailed t-tests (significance level: **p < 0.01; ***p < 0.001).

Note: Complete absence of RdRp trajectories might be resolved using one of the presented solutions (Troubleshooting; Problem 4: no RdRp activity observed).

EXPECTED OUTCOMES

The magnetic tweezers protocol presented here enables a quantitative description of RdRp RNA synthesis dynamics, including the nucleotide incorporation rate, pausing frequency, and pause lifetimes, which can be probed under a variety of conditions. The presented data show the detectable changes in RNA synthesis processivity and pausing dynamics in presence of pyrazine carboxamide nucleotide analog T-1106 (Figures 8 and 9). The application of this method to variations in conditions, such as NTP concentration, different nucleotide analogs, or even transient roadblocks imposed by RNA-binding proteins, will allow the identification and quantitative characterization of their effect on RdRp translocation and RNA synthesis dynamics. Figures related to the expected outcome of each step of the protocol have been presented.

QUANTIFICATION AND STATISTICAL ANALYSIS

In this section, the protocol describes the analysis of the bead z-displacement (associated with ssRNA displacement during RNA synthesis) obtained in the MT experiment in a step-wise fashion. In the first step, the z-displacement of the magnetic bead is converted into number of nucleotides synthesized, from which the RdRp processivity and the average velocity are calculated. In the last step the protocol guides through the process of constructing the dwell time distributions of the RNA synthesis kinetics, from which the average pause lifetimes and pausing probabilities are extracted. As aforementioned, we used Igor Pro (V6.37) as software platform for the analysis of the RdRp trajectories, however, scripting-capable software that is able to import the delimited text file output from the acquisition software (e.g., MATLAB or Python) is equally suited.

Converting changes in RNA extension to nucleotides synthesized

© Timing: 1 h

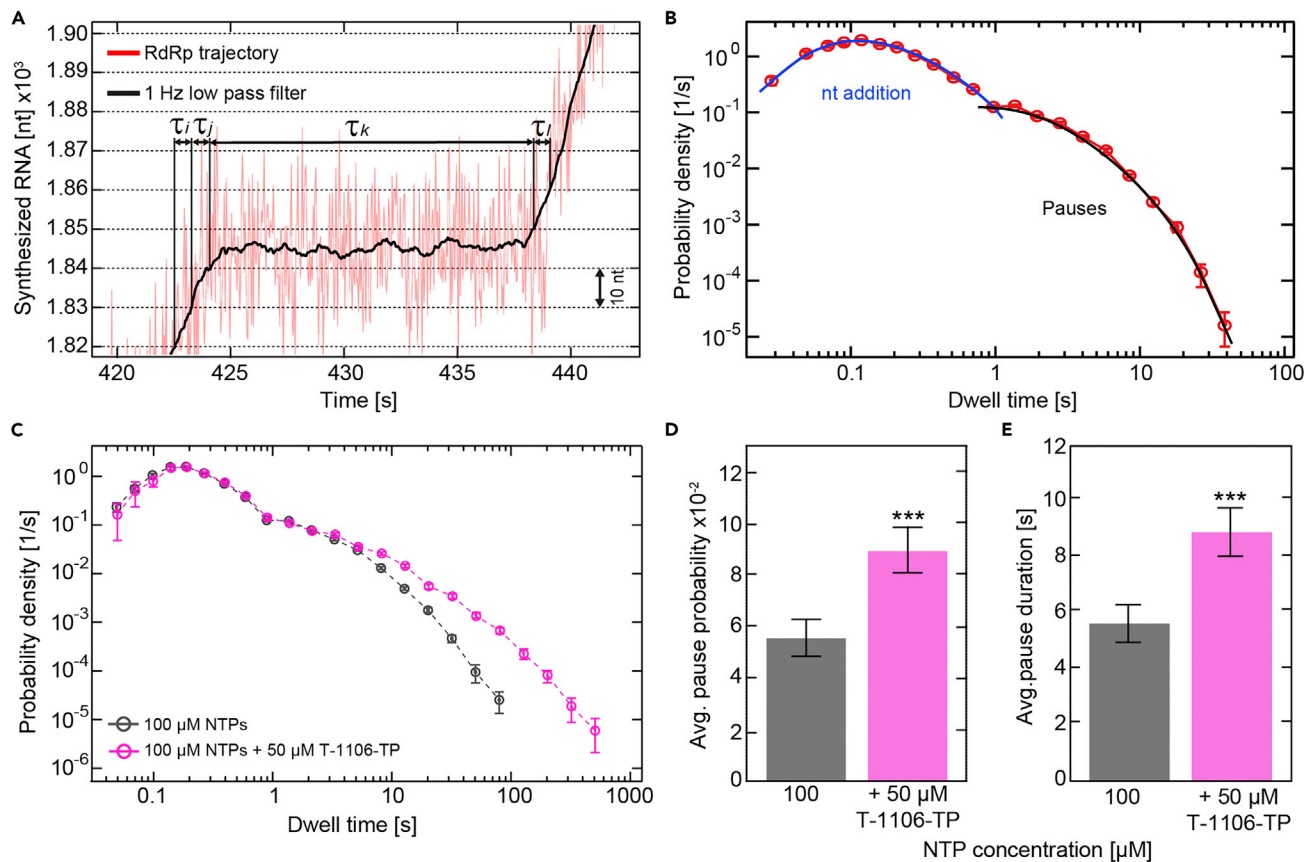


Figure 9. Constructing the dwell time distribution and extracting pausing dynamics of EV-A71 RdRp RNA synthesis

(A) Magnified region of the individual RNA synthesis trajectory shown in Figure 7A. The dwell times are determined by extracting the time (τ_i) needed for the RdRp to synthesize a defined number of consecutive nucleotides; the example shows ten-nucleotide dwell time windows as dashed lines.

(B) Dwell time probability distribution of 9,981 dwell times extracted from RNA synthesis trajectories using a dwell time window of four nucleotides and binned with six bins per decade. The error bars (AVG \pm SD) result from bootstrapping with 1,000 iterations. Solid curves show the best fit of a simple model to the data, where the contributions of individual components of the model are separated: the blue curve at short timescales captures the effective pause-free elongation rate, while the black curve corresponds to a single pause state with exponential decay.

(C) Superimposed dwell time distributions of EV-A71 RdRp in absence (gray) and presence (magenta) of the nucleotide analog T-1106 triphosphate; data sets from (Janissen et al., 2021).

(D and E) Quantification of the dwell time distributions in (C): the addition of T-1106 triphosphate (magenta) induces a significant increase in (D) pausing probability (mean \pm SD) and (E) average pause duration (mean \pm SEM). Statistical analyses were performed using unpaired, two-tailed t-tests (significance level: *** p < 0.001).

1. For each individual RdRp trajectory, normalize the RNA extension to the extension before the addition of NTPs. Next, cut out the lag time and final plateaus where there is no RdRp synthesis activity or dissociation has occurred (see Figures 7B and 7C).
2. Convert the ssRNA extension to the number of RNA nucleotides synthesized, NT_{synth} , using the formula below, where Δl_{meas} represents the measured apparent increase in RNA length, and $l_{\text{ss}}(F) - l_{\text{ds}}(F)$ is the difference in length between the extensions of ssRNA and dsRNA:

$$\alpha = (l_{\text{ss}}(F) - l_{\text{ds}}(F))^{-1}$$

$$NT_{\text{synth}} = \alpha * \Delta l_{\text{meas}}$$

Extracting RdRp processivity and average RNA synthesis velocity

© Timing: 1 h

- Determine the average RdRp processivity from the maximum amount of RNA synthesized in each individual trajectory (*nucleotides_i*; example shown in [Figure 8A](#)):
- Compute the average velocity by dividing individual RdRp processivities (step 3) by the duration of active RNA synthesis (example shown in [Figure 8B](#)):

$$V_{\text{average}} \left(\frac{\text{nt}}{\text{s}} \right) = \frac{\sum_{i=1}^n \frac{\text{nucleotides}_i (\text{nt})}{\text{time}_i (\text{s})}}{n}$$

Constructing the dwell time distribution and extracting average pause lifetimes and pausing probability

⌚ Timing: 1 h

The construction of the dwell time distribution allows for the calculation of both the average pause probability as well as the average pause lifetime. The dwell times are determined by extracting from all RNA synthesis trajectories the time needed for the RdRp to synthesize a defined number of consecutive nucleotides ([Dulin et al., 2015c](#)).

- Filter the individual RNA synthesis trajectories using a 1 Hz sliding mean filter.
- Construct a dwell time distribution ([Figures 9A–9C](#)) of all the RNA synthesis trajectories belonging to the same experimental condition. You may use the MATLAB script provided in a repository (<https://doi.org/10.4121/19145426>), which also includes example data.
- From the dwell time distribution, determine the lifetime where pausing starts. In the example shown in [Figures 9B and 9C](#), the lower bound of pausing lifetimes is > 1 s.
- Calculate the average pause probability P_{pause} by integrating dwell times larger than the pause lifetime lower bound (see example in [Figure 9D](#)):

$$\bar{P}_{\text{pause}} = \frac{\sum_{i=1}^n P_{\text{pause}, i}}{n}$$

- Determine the average pause lifetime by averaging all dwell times larger than the pause lifetime lower bound (see example in [Figure 9E](#)):

$$\bar{\tau}_{\text{pause}} (\text{s}) = \frac{\sum_{i=1}^n \tau_i (\text{s})}{n}$$

LIMITATIONS

A limitation of the presented method is the inability to directly interrogate the RNA products of RdRp activity that are produced in the magnetic tweezers. In addition, the amount of processing power required to determine many tracked bead positions using Z-lookup table cross-correlation can be significant. To avoid crashing or freezing of the software, it is advised to ensure that a PC with sufficient computational power is used for tracking of many magnetic beads.

TROUBLESHOOTING

Problem 1

The flow cell leaks.

Potential solution

- Reduce the inlet and outlet holes' diameter in the top cover slip (step 1).
- Tighten carefully the screws of the flow cell (step 10).
- Check O-rings for graining or damage of the rubber and possibly replace them (step 10).

- Replace the flow cell in the holder (step 10).
- Check attachment of inlet and outlet tubing (step 11).

Problem 2

Absence of tether formation.

Potential solution

- Replace stocks of anti-DIG, RNA construct, RNase inhibitor, and magnetic beads (steps 17, 28, and 31).
- Use or synthesize a new RNA construct. Contaminations with RNases can cut the dsRNA, thus preventing tether formation (step 28).
- Increase RNA concentration (step 28).
- Increase incubation time of magnetic beads (step 31).

Problem 3

All magnetic beads are adhered to the surface.

Potential solution

- Increase passivation time of the flow cell (step 20).
- Use new magnetic bead stock. Make sure magnetic beads are not expired (step 25).
- Switch hydrophobicity of the beads (from M280 to M270 or vice versa) (step 25).
- Increase passivation time of the magnetic beads (step 26).
- Reduce incubation time of the magnetic beads (step 31).
- Give a short pulse of high force (max. 40 pN) to break non-specific bead adhesion (prior to step 46).

Problem 4

No RdRp activity observed.

Potential solution

- Use another batch of or purify new RdRp (step 37).
- Increase ternary complex formation time (step 38).
- Increase the concentration of rNTPs (step 47).

Problem 5

Output parameters differ significantly between experiments with the same conditions.

Potential solution

- Exclude outliers (step 1).
- Ensure that the cropping of the RdRp trajectory is performed correctly: directly after the lag phase and right before reaching the final plateau (step 1).
- Ensure that all used materials (e.g., RNA, nucleotides, RdRp, buffers, etc.) are from the same batch and within expiration dates (steps 28 and 47).

RESOURCE AVAILABILITY

Lead contact

Further information and requests for resources and reagents should be directed to and will be fulfilled by the lead contact, Nynke H. Dekker (N.H.Dekker@tudelft.nl).

Materials availability

This study did not generate new unique reagents.

Data and code availability

We did not generate any new datasets. The original data can be found under previously published (Janissen et al. (2021)) (Janissen et al., 2021) (Janissen et al., 2021) (Janissen et al., 2021). The dwell time distribution code (MATLAB) is available at the 4TU Research Data repository (<https://doi.org/10.4121/19145426>).

ACKNOWLEDGMENTS

We acknowledge funding to N.H.D. from the Human Frontiers Science Program (RPG0011/2015). We thank Kaley McCluskey for a critical reading of the manuscript.

AUTHOR CONTRIBUTIONS

L.K. and R.J. conceived the manuscript. L.K. and R.J. performed and analyzed the single-molecule experiments. T.v.L. synthesized the RNA template constructs. L.K., R.J., and N.H.D. wrote the manuscript.

DECLARATION OF INTERESTS

The authors declare no competing interests.

REFERENCES

- Cnossen, J.P., Dulin, D., and Dekker, N.H. (2014). An optimized software framework for real-time, high-throughput tracking of spherical beads. *Rev. Sci. Instrum.* *85*, 103712.
- Dulin, D., Vilfan, I.D., Berghuis, B.A., Hage, S., Bamford, D.H., Poranen, M.M., Depken, M., and Dekker, N.H. (2015a). Elongation-competent pauses govern the fidelity of a viral RNA-dependent RNA polymerase. *Cell Rep.* *10*, 983–992.
- Dulin, D., Vilfan, I.D., Berghuis, B.A., Poranen, M.M., Depken, M., and Dekker, N.H. (2015b). Backtracking behavior in viral RNA-dependent RNA polymerase provides the basis for a second initiation site. *Nucleic Acids Res.* *43*, 10421–10429.
- Dulin, D., Berghuis, B.A., Depken, M., and Dekker, N.H. (2015c). Untangling reaction pathways through modern approaches to high-throughput single-molecule force-spectroscopy experiments. *Curr. Opin. Struct. Biol.* *34*, 116–122.
- Fields, B.N., Knipe, D.M., and Howley, P.M. (1996). *Fields Virology* (Lippincott-Raven Publishers).
- Gosse, C., and Croquette, V. (2002). Magnetic tweezers: micromanipulation and force measurement at the molecular level. *Biophys. J.* *82*, 3314–3329.
- Janissen, R., Woodman, A., Shengjuler, D., Vallet, T., Lee, K.-M., Kuijpers, L., Moustafa, I.M., Fitzgerald, F., Huang, P.-N., Perkins, A.L., et al. (2021). Induced intra- and intermolecular template switching as a therapeutic mechanism against RNA viruses. *Mol. Cell* *81*, 4467–4480.e7.
- Klaue, D., and Seidel, R. (2009). Torsional stiffness of single superparamagnetic microspheres in an external magnetic field. *Phys. Rev. Lett.* *102*, 028302.
- Lipfert, J., Hao, X., and Dekker, N.H. (2009). Quantitative modeling and optimization of magnetic tweezers. *Biophys. J.* *96*, 5040–5049.
- Ostrofet, E., Papini, F.S., and Dulin, D. (2018). Correction-free force calibration for magnetic tweezers experiments. *Sci. Rep.* *8*, 17811.
- Seifert, M., Bera, S.C., van Nies, P., Kirchdoerfer, R.N., Shannon, A., Le, T.-T.-N., Meng, X., Xia, H., Wood, J.M., Harris, L.D., et al. (2021). Inhibition of SARS-CoV-2 polymerase by nucleotide analogs from a single-molecule perspective. *Elife* *10*, e70968.
- Yu, Z., Dulin, D., Cnossen, J., Köber, M., van Oene, M.M., Ordu, O., Berghuis, B.A., Hensgens, T., Lipfert, J., and Dekker, N.H. (2014). A force calibration standard for magnetic tweezers. *Rev. Sci. Instrum.* *85*, 123114.